

## Article

# Selection of Design Scheme for an Ultrahigh-Pressure Hydrostatic Extrusion Cylinder

Jian Yang <sup>1,2</sup>, Lei Zhang <sup>1,\*</sup>, Jun Zhang <sup>2</sup>, Hao Wang <sup>1</sup>, Dong Zhang <sup>1</sup>, Yuanxin Luo <sup>1</sup> and Yongqin Wang <sup>1</sup>

<sup>1</sup> College of Mechanical and Vehicle Engineering, Chongqing University, Chongqing 400044, China; yjxjtu@163.com (J.Y.); wanghao33@cqu.edu.cn (H.W.); dongzhang@cqu.edu.cn (D.Z.); yxluo@cqu.edu.cn (Y.L.); wyq@cqu.edu.cn (Y.W.)

<sup>2</sup> The State Key Laboratory of Metal Extrusion and Forging Equipment Technology, China Heavy Machinery Research Institute Inc., Xi'an 710018, China; chungjun@163.com

\* Correspondence: lzhang@cqu.edu.cn

**Abstract:** In this study, the mechanical models of a multilayer combined extrusion cylinder and a steel-wire-winding extrusion cylinder were established and compared using a finite element simulation and existing experimental cases. This work provides theoretical support for the selection of an ultrahigh-pressure extrusion cylinder. Comparative analysis of an ultrahigh-pressure extrusion structure was carried out. The mathematical optimization model is established based on the mechanical model, and the ultimate bearing capacities of the schemes are compared. Additionally, the winding mode and the number of core layers of the extrusion cylinder are compared and analyzed, which provides a theoretical basis for the parameter design of the steel-wire-winding ultrahigh-pressure extrusion cylinder. This work holds good theoretical significance and practical value for the promotion and application of ultrahigh-pressure hydrostatic extrusion technology.

**Keywords:** multilayer combined extrusion cylinder; mathematical optimization model; steel-wire-winding extrusion cylinder; ultrahigh-pressure hydrostatic extrusion cylinder



**Citation:** Yang, J.; Zhang, L.; Zhang, J.; Wang, H.; Zhang, D.; Luo, Y.; Wang, Y. Selection of Design Scheme for an Ultrahigh-Pressure Hydrostatic Extrusion Cylinder. *Actuators* **2023**, *12*, 369. <https://doi.org/10.3390/act12100369>

Academic Editor: Tatiana Minav

Received: 16 August 2023

Revised: 13 September 2023

Accepted: 20 September 2023

Published: 25 September 2023



**Copyright:** © 2023 by the authors. Licensee MDPI, Basel, Switzerland. This article is an open access article distributed under the terms and conditions of the Creative Commons Attribution (CC BY) license (<https://creativecommons.org/licenses/by/4.0/>).

## 1. Introduction

Hydrostatic extrusion offers the advantages of low extrusion pressure, less die wear, uniform material deformation, high-dimensional precision for extruded products, and smooth surfaces. This method is widely used in the extrusion processing of different profiles of high-temperature alloys and materials that are difficult to process. However, ultrahigh-pressure (>1000 MPa) extrusion is the main method used to process refractory alloys, such as tungsten alloys. At present, there are relatively few instances of the production application of ultrahigh-pressure hydrostatic extrusion technology, which is mainly due to there being limited research on the design mechanism and selection of ultrahigh-pressure extrusion cylinders. Ultrahigh-pressure extrusion cylinders are some of the core components of ultrahigh-pressure hydrostatic extrusion technology. They are the basis for guaranteeing a smooth extrusion process, and they incur huge losses and have high costs. Therefore, the reasonable design of an extrusion cylinder holds great significance as it could ensure production and reduce product costs.

Few studies, however, have examined ultrahigh-pressure extrusion cylinders with internal pressures greater than 1000 MPa, and many research studies on extrusion cylinders have focused mainly on the basic design theories of extrusion cylinders. For example, Horne [1] applied the elastic–plastic theory to analyze the stress–strain distribution of an extrusion cylinder. Zhao and Liu [2] systematically summarized their practical experience with aluminum alloy extrusion tools and proposed the concept of the optimal design of an extrusion cylinder. Ao and Wang [3] provided a calculation idea for determining the size parameters of an extrusion cylinder and the interference amount between each layer of the cylinder based on the double-shear strength theory. Wang and Liu [4] and Li et al. [5]

conducted a numerical simulation of the stress state of a multilayer preloaded circular extrusion cylinder and obtained the deformation and stress distribution law of the extrusion cylinder. Tang et al. [6] systematically studied the basic methods for the material selection, structural design, and strength check of an extrusion cylinder and simplified the calculation principles of an extrusion cylinder. Xiong [7] discussed the stress and deformation law of an autofrettage combined extrusion cylinder to provide support for improving the design and service conditions of the extrusion cylinder. Song [8] calculated the interfacial force of each layer of a multilayer combined extrusion cylinder by combining the calculation formulas for the stress distribution of a thick-wall cylinder and the deformation coordination condition. Li [9] and Ma [10] conducted an in-depth study of the design theory and service life of an extrusion cylinder and proposed a life prediction model for an extrusion cylinder based on the interaction between the fatigue and the creep.

For steel-wire-winding extrusion cylinder, Wu et al. [11] proposed a design method for a steel-wire-winding split-assembled combined extrusion cylinder that greatly reduced the manufacturing difficulty compared with an integral extrusion cylinder and took into account the economic cost. Yang et al. [12] made some improvements based on this by changing the core cylinder to have an oblique end face instead of a flat end face, which made the steel-wire-winding split-assembled combined extrusion cylinder lighter in weight and stronger in terms of its preloading ability, and further reduced the manufacturing cost of the extrusion cylinder. Chi and Cao [13] studied the effect of the steel wire prestress on the inner wall of an extrusion cylinder, and discussed the relationship between the geometric size of the extrusion cylinder, the number of steel wire layers, and the steel wire prestress. Liu et al. [14] proposed two design schemes to address the phenomena of steel wire creep and stress relaxation at high temperatures and verified the schemes through tests, providing ideas for solving the preheating and heat insulation problems of a steel-wire-winding extrusion cylinder.

For other relevant research studies, Knut Vedeld et al. [15] developed an analytical solution for the displacement field and corresponding stress state in multi-layer cylinders subjected to pressure and thermal loading to solve the Stresses in heated pressurized multi-layer cylinders in generalized plane strain conditions. Sollund Havar et al. [16] derived the analytical solutions for calculating the displacement and stress of two independent multilayer elastic cylinders under pressure and thermal loads for efficient analysis of heated and pressurized multi-layer cylinders. Zhe Zhang et al. [17] used two different die designs under the same extrusion conditions to conduct numerical studies on metal flow characteristics, extrusion pressure, welding quality and billet utilization. Zhe Zhang et al. [18] thought that extrusion is a very promising technology in the production of wide aluminum stiffened panels, an focus on the analysis of ways to widen the stiffened plates in the extrusion process, such as stretch extrusion and late flattening after extrusion.

Fewer production applications are available for ultrahigh-pressure hydrostatic extrusion, which is mainly due to the cylinder, and the design mechanism for handling ultrahigh pressure is limited. Besides, Steel wire winding extrusion cylinder and multi-layer extrusion cylinder have their applicable strength range and use scenarios, and can be selected according to demand. Ultrahigh-pressure cylinder design analysis system research methods and comparative analyses of super-high-pressure cylinder designs and structures are key technologies for the popularization and application of ultrahigh-pressure hydrostatic extrusion technology, which holds great theoretical guiding significance and practical value.

In the next section, we consider the mechanical model of a multilayer combined extrusion cylinder and a wire-winding extrusion cylinder. Section 3 verifies the theoretical model according to a comparison of the theoretical results with the finite element simulation and experimental results. In Section 4, based on the mechanical model, the mathematical optimization model is established and the ultimate bearing capacity of each scheme is compared. Additionally, the winding mode and the number of layers of the core cylinder are compared and analyzed. Finally, the main conclusions are summarized in Section 5.

## 2. Theoretical Model

In the early stage of development, the extrusion cylinder mainly had a single-layer cylinder structure for the extrusion process and a low internal pressure. This structure bears internal pressure only when at work, and the maximum radial stress and tangential stress appear in the inner wall of the extrusion cylinder. The radial stress is compressive and the tangential stress is tensile, which leads to the easy destruction of the inner wall. Even with the use of high-quality materials with a high allowable strength, the extrusion cylinder still requires a great wall thickness, which increases the difficulty of manufacturing it, among other aspects. Additionally, it is difficult to repair the cylinder after damage or wear.

Since the introduction of the concept of a prestressed extrusion cylinder, the structure of the extrusion cylinder has been developed. This structure is used in multilayer combined extrusion cylinders and steel-wire-winding extrusion cylinders. In both cases, the prestress applied on the outside of the lining partially or completely offsets the tangential tensile stress generated by the internal pressure to improve the bearing capacity of the extrusion cylinder. Because of the radial compression of the outside pressure, the tangential stress is compressive stress, which can compensate for the tangential stress when the lining is subjected to internal pressure. Therefore, for the prestressed extrusion cylinder, the tangential stress can be reduced or even dropped to zero with a reasonable adjustment of the value of the external pressure. Thus, the extrusion cylinder can have a higher bearing capacity, effectively preventing the longitudinal cracking of the extrusion cylinder and extending its life [19].

In summary, compared with the two types of prestressed extrusion cylinders, the single-layer cylinder has a poor bearing capacity and a potential that is too low to withstand ultrahigh pressure. Therefore, this paper discusses the design of an ultrahigh-pressure extrusion cylinder structure that can be mainly utilized in multilayer combined extrusion cylinders and steel-wire-winding extrusion cylinders.

### 2.1. Mechanics Model of Multilayer Combined Extrusion Cylinder

When studying the stress distribution of a multilayer combined extrusion cylinder, it is often necessary to make some simplifications to facilitate the analysis and calculation. The assumptions in this study are as follows:

1. Each layer of the extrusion cylinder meets the requirement of having a thick wall, and the ratio of the outer diameter to the inner diameter is greater than 1.1.
2. Regardless of the effect of the end structure of the extrusion cylinder, the extrusion cylinder body is regarded as an ideal hollow cylinder, and the load is axisymmetrically distributed accordingly.
3. There is no torsion and axial bending of the extrusion cylinder in the process of extrusion, and the cylinder is circular before and after deformation under a load.
4. The axial stress caused by the friction between the billet or the extrusion shaft and the inner cylinder in the extrusion process is ignored.

Therefore, the stress analysis problem of a multilayer composite extrusion cylinder can be simplified to the problem of axisymmetric plane strain. Based on the Lamé formula and combined with the deformation coordination conditions, Luo et al. [20] derived the DDM method for calculating the interfacial forces at the mating surface of a multilayer extrusion cylinder and then obtained the stress–strain distribution of each layer of the extrusion cylinder.

Within the elastic range, the radial stress  $\sigma_r$  and tangential stress  $\sigma_t$  at a point where the inner distance of each layer of the cylinder is  $r$  from the axis can be calculated with the Lamé formula (Equation (1)). For the  $i$ -th layer of the cylinder, there is

$$\begin{cases} \sigma_{ri} = \frac{P_{i,in}r_{i,in}^2}{r_{i,out}^2 - r_{i,in}^2} \left(1 - \frac{r_{i,out}^2}{r^2}\right) - \frac{P_{i,out}r_{i,out}^2}{r_{i,out}^2 - r_{i,in}^2} \left(1 - \frac{r_{i,in}^2}{r^2}\right) \\ \sigma_{ti} = \frac{P_{i,in}r_{i,in}^2}{r_{i,out}^2 - r_{i,in}^2} \left(1 + \frac{r_{i,out}^2}{r^2}\right) - \frac{P_{i,out}r_{i,out}^2}{r_{i,out}^2 - r_{i,in}^2} \left(1 + \frac{r_{i,in}^2}{r^2}\right) \end{cases} \quad (1)$$

where  $P_{i, in}$  and  $P_{i, out}$  are the internal pressure and the external pressure of the  $i$ -th layer cylinder, respectively.

According to Equation (1), because of the effect of the internal pressure and external pressure, the inner and outer diameters of the  $i$ -th layer ( $i = 1, 2 \dots, n$ ) are deformed, and the inner and outer deformations are  $u_{i, in}$  and  $u_{i, out}$ , respectively. The calculation formula is as follows [21]:

$$\begin{cases} u_{i, in} = \frac{1}{E_i} \left[ (1 - \mu_i) A_i r_{i, in} + (1 + \mu_i) \frac{B_i}{r_{i, in}} \right] \\ u_{i, out} = \frac{1}{E_i} \left[ (1 - \mu_i) A_i r_{i, out} + (1 + \mu_i) \frac{B_i}{r_{i, out}} \right] \end{cases} \quad (2)$$

where  $A_i = \frac{P_{i, in} r_{i, in}^2 - P_{i, out} r_{i, out}^2}{r_{i, out}^2 - r_{i, in}^2}$ ,  $B_i = \frac{r_{i, in}^2 r_{i, out}^2 (P_{i, in} - P_{i, out})}{r_{i, out}^2 - r_{i, in}^2}$ ,  $\mu_i$  is the Poisson ratio of the  $i$ -th layer, and  $E_i$  is the elastic modulus of the  $i$ -th layer. Because the radial stress must be continuous, for the interface force of the extrusion cylinder

$$P_{i-1, out} = P_{i, in}, \quad (3)$$

and the mating surface between each layer and cylinder meets the following displacement coordination conditions:

$$R_{i, out} + u_{i, out} = R_{i+1, in} + u_{i+1, in} \quad i = 1, 2, 3, \dots, n - 1 \quad (4)$$

Thus, for the conditions of the known inner and outer diameters ( $r_{i, in}$  and  $r_{i, out}$ ) and the material parameters  $E_i$  and  $\mu_i$ , the strain coordination equation (Equation (2)) and the condition equation (Equation (4)) can be used to calculate the internal and external deformation of the  $i$ -th layer cylinder ( $P_{i-1, i}$  and  $P_{i, i+1}$ ), and the stress-strain distribution of the  $i$ -th layer cylinder can be obtained.

## 2.2. Mechanics Model of Steel-Wire-Winding Extrusion Cylinder

For the mechanical model of a steel-wire-winding extrusion cylinder, Wang et al. [22] proposed a stress prediction model for calculating the stress of steel wire in the crimping process, which provided a good reference for the design and calculation of steel-wire-winding extrusion cylinders. By improving upon this method in this study, the improved method can be used to calculate the stress and strain distribution of the steel wire layer of the extrusion cylinder. To simplify the stress analysis and calculation of the steel wire layer, the following assumptions are made:

1. The load and deformation of the steel wire have a linear relationship, that is, linear elasticity.
2. The steel wire is isotropic.
3. The influence of the initial winding section on the subsequent steel wire is ignored, and it is assumed that each layer of the steel wire is a thin-walled cylinder connected end to end.
4. The steel wire layer is not subject to an axial load.
5. The steel wire layer is round before and after being loaded and deformed.

Therefore, the steel-wire-winding extrusion cylinder can be simplified into a multilayer prestressed cylinder in which the steel wire layer is under tension. The force analysis diagram is shown in Figure 1. Similarly, the Lamé formula and the DDM method can be applied to the calculation of the steel wire layers.

As shown in Figure 2, it is assumed that the core cylinder with the inner diameter  $R_{11}$  and the outer diameter  $R_{12}$  is wrapped in the first layer of steel wire (inner diameter  $R_{21}$ , thickness  $h$ , and tension  $N$ ). After the assembly is completed, the inner and outer diameters of the two layers are deformed to  $r_{1in}$ ,  $r_{1out}$ ,  $r_{2in}$ , and  $r_{2out}$ , where  $r_{1out} = r_{2in}$ .

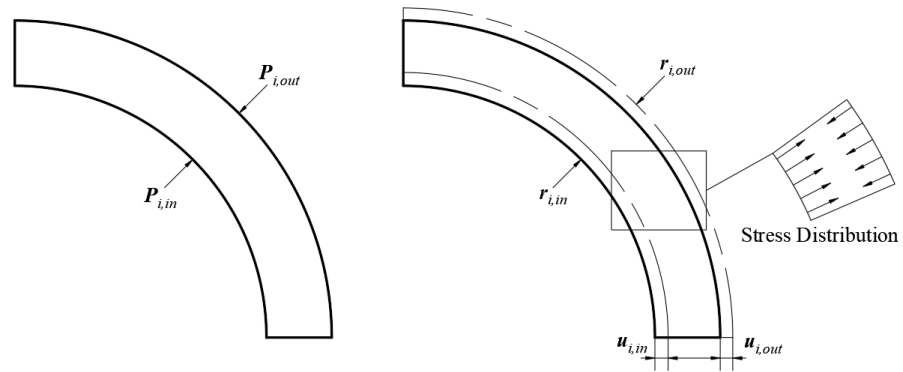


Figure 1. Force, deformation, stress resultants and couples diagram of the  $i$  layer.

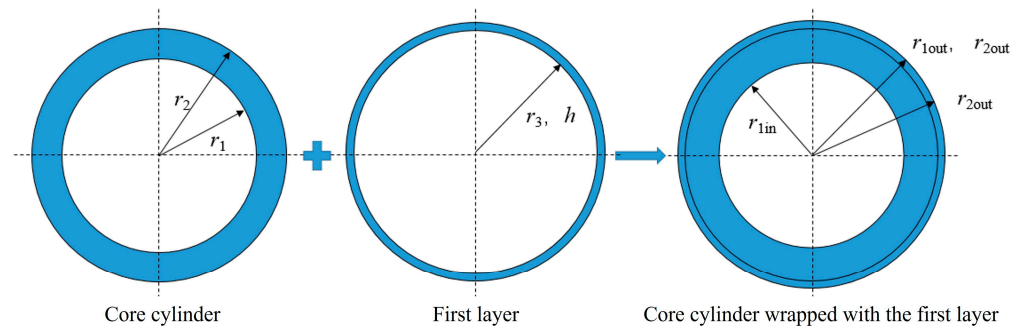


Figure 2. Schematic diagram of wire-winding deformation of the first layer.

For the first layer of steel wire before deformation,  $R_{22} = R_{21} + h_g$ , and then the mechanics model can be established according to the DDM method proposed by Luo et al. [20].

Similarly, the multilayer steel-wire-winding model can be regarded as a combination of the last layer and the whole inner cylinder. Therefore, the iterative method is adopted, and the deformation of each layer of the steel wire needs to be reanalyzed every time a layer of steel wire is wound.

$$\begin{cases} P_{n-1,n} = \frac{R_{n1}^2 - R_{11}^2}{R_{n1}^2} \left( \frac{\sigma_{0n}}{2} \ln \frac{R_{n2}^2 - R_{11}^2}{R_{n1}^2 - R_{11}^2} \right) - P_{01} \frac{R_{11}^2}{R_{n2}^2 - R_{11}^2} \left( 1 - \frac{R_{n2}^2}{R_{n1}^2} \right) \\ r_{i1} - R_{i1} = \frac{1}{E(R_{i2}^2 - R_{i1}^2)} \left[ (P_{i-1,i} R_{i1}^2 - P_{i,i+1} R_{i2}^2) (1 - \mu) R_{i1} \right. \\ \quad \left. - R_{i1}^2 R_{i2}^2 (P_{i,i+1} - P_{i-1,i}) (1 + \mu) \frac{1}{R_{i1}} \right], i = 1, 2, 3, \dots, n \\ r_{i2} - R_{i2} = \frac{1}{E(R_{i2}^2 - R_{i1}^2)} \left[ (P_{i-1,i} R_{i1}^2 - P_{i,i+1} R_{i2}^2) (1 - \mu) R_{i2} \right. \\ \quad \left. - R_{i1}^2 R_{i2}^2 (P_{i,i+1} - P_{i-1,i}) (1 + \mu) \frac{1}{R_{i2}} \right], i = 1, 2, 3, \dots, n \\ r_{i2} = r_{i+1,1}, i = 1, 2, 3, \dots, n - 1 \end{cases} \quad (5)$$

where  $R_{i1}$  is the inner radius of the  $i$ -th layer (core cylinder) before assembly (deformation),  $R_{i2}$  is the outer radius of the  $i$ -th layer before assembly (deformation),  $r_{i1}$  is the inner radius of the  $i$ -th layer after assembly,  $r_{i2}$  is the outer radius of the  $i$ -th layer after assembly,  $P_1$  is the pressure on the inner wall of the first layer,  $P_{i-1,i}$  is the interface force between the  $(i - 1)$ -th layer and the  $i$ -th layer after assembly,  $P_{i,i+1}$  is the interface force between the  $i$ -th layer and the  $i + 1$ -th layer after assembly, and  $P_{n,n-1}$  is the interface force between the  $n$ -th layer and the  $(n - 1)$ -th layer after assembly.

For the extrusion cylinder wound with  $n$  layers of steel wire there are a total of  $3n$  equations, based on which the stress distribution of the extrusion cylinder and the radial displacement value of each layer can be solved.

### 3. Verification of Theoretical Model

#### 3.1. Verification of Multilayer Combined Extrusion Cylinder Mechanics Model with Numerical Simulation

Taking the most widely used three-layer combined extrusion cylinder as an example, the finite element analysis software ABAQUS is used to compare and analyze the mechanical model of the multilayer combined extrusion cylinder described earlier.

The size of the inner cylinder is set to 110–168 mm. The size of the middle cylinder is 167.664–213 mm, the size of the outer cylinder is 212.574–450 mm, and the inner pressure is set to 700 MPa. Assuming that the elastic modulus and the Poisson ratio of each layer are equal,  $E$  is 210,000 MPa,  $\mu$  is 0.3, and the interference coefficient between each layer is 2.0%. The calculation results show that the interference between the inner and middle cylinders is 0.336 mm and the interference between the outer and inner cylinders is 0.426 mm. Figures 3 and 4 show the finite element analysis results of the radial stress and the tangential stress in the prestressed state and the combined state, respectively.

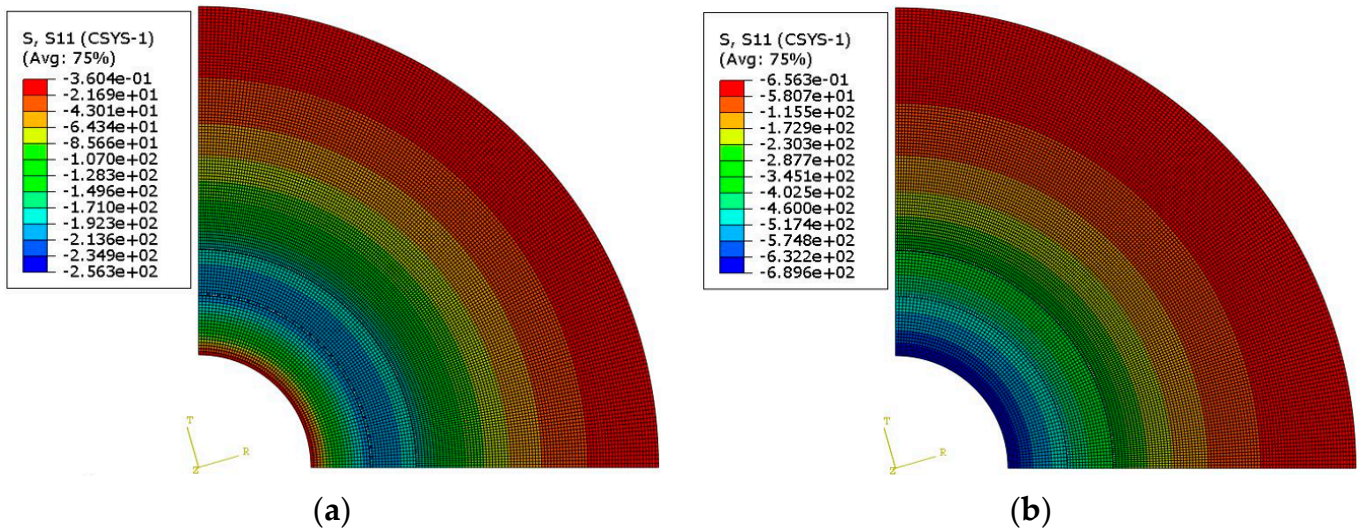


Figure 3. Radial stress distribution of cylinder: (a) preload state; (b) composite state.

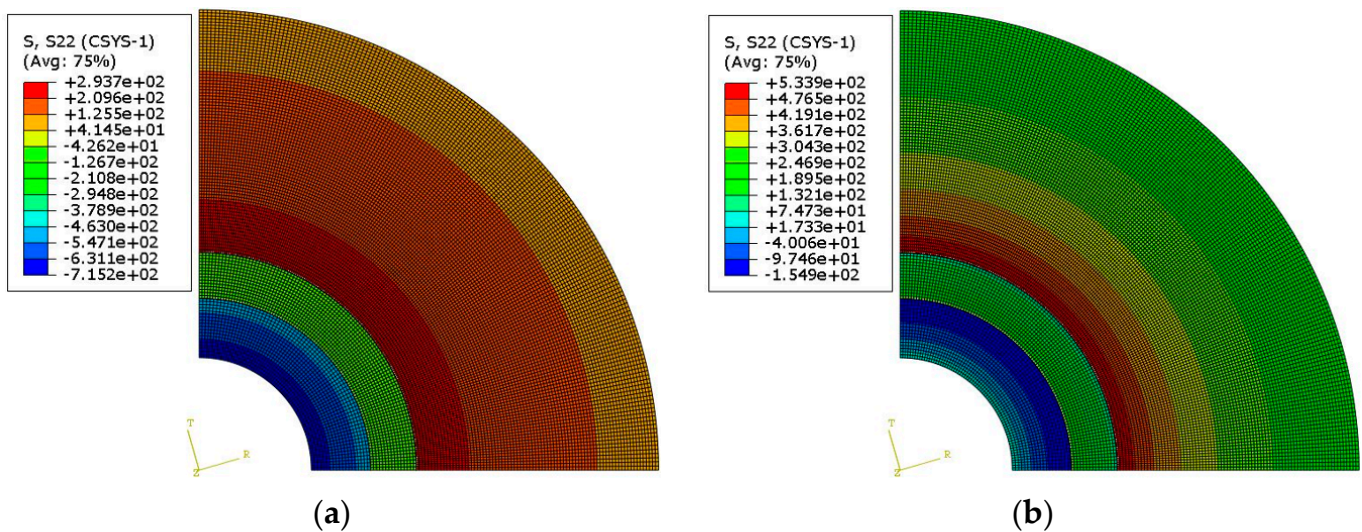


Figure 4. Tangential stress distribution of cylinder: (a) preload state; (b) composite state.

The results of the finite element analysis are compared with those calculated with the mechanical model at each interface. Tables 1 and 2 display the values of the radial stress and the tangential stress in the preloaded state and the combined state. It can be seen that

the mechanical model calculation results are in good agreement with the finite element results, which proves that the model is reliable.

**Table 1.** Comparison of mechanical model and finite element results in preload state.

Node Location of All Sections		Mechanics Model		Finite Element Method	
		Radial Stress/MPa	Tangential Stress/MPa	Radial Stress/MPa	Tangential Stress/MPa
First layer	$r_{in}$	0	−729.5735	−9.8702	−715.2059
	$r_{out}$	−208.3919	−521.1756	−208.1870	−522.4084
Second layer	$r_{in}$	−208.3979	−103.5567	−208.1870	−110.1769
	$r_{out}$	−188.5881	−123.3665	−186.6860	−120.7337
Third layer	$r_{in}$	−188.5881	297.4915	−186.6860	290.0079
	$r_{out}$	0	108.9034	−0.3605	108.2561

**Table 2.** Comparison of mechanical model and finite element results in composite state.

Node Location of All Sections		Mechanics Model		Finite Element Method	
		Radial Stress/MPa	Tangential Stress/MPa	Radial Stress/MPa	Radial Stress/MPa
First layer	$r_{in}$	−700	56.0874	−689.61	52.7487
	$r_{out}$	−484.0286	−159.8840	−499.419	−147.2651
Second layer	$r_{in}$	−484.0286	261.5109	−499.419	247.8924
	$r_{out}$	−343.1585	120.6408	−337.935	127.4488
Third layer	$r_{in}$	−343.1585	541.3212	−337.935	529.0016
	$r_{out}$	0	198.1628	−0.65635	197.1195

### 3.2. Verification of the Steel-Wire-Winding Extrusion Cylinder Mechanics Model through Experimental Comparison

To determine the radial shrinkage of the steel-wire-winding extrusion cylinder, the results of existing experimental cases are used for comparison. The Xi'an Heavy Machinery Research Institute used strain gauges in the article "Research on Hydrostatic Extrusion Equipment" to perform related test experiments on steel-wire-winding extrusion cylinders. In this study, the radial shrinkage is calculated using the mechanical model of the steel-wire-winding extrusion cylinder described in Section 2.2, which is compared with that from other studies and analyzed to verify the radial shrinkage of the steel-wire-winding extrusion cylinder. Two sets of models mentioned in the literature are listed, and the parameters are as follows:

1. The inner diameter of the inner cylinder is  $\varphi 75$  mm, the outer diameter is  $\varphi 120$  mm, the steel wire tension  $T = 2570$  N, the material elastic modulus  $E = 205$  GPa, Poisson's ratio  $\mu = 0.3$ , and the steel wire thickness is 1 mm. In addition, the number of steel wire layers wound is 10, 20, 30, 40, 50, 60, and 70.
2. The inner diameter of the inner cylinder is  $\varphi 60$  mm, the outer diameter is  $\varphi 100$  mm, the steel wire tension  $T = 2800$  N, the material elastic modulus  $E = 205$  GPa, Poisson's ratio  $\mu = 0.3$ , and the steel wire thickness is 1 mm. In addition, the number of layers of wound steel wires is 10, 20, 30, 44, 54, 64, 74, 84, 92, and 96.

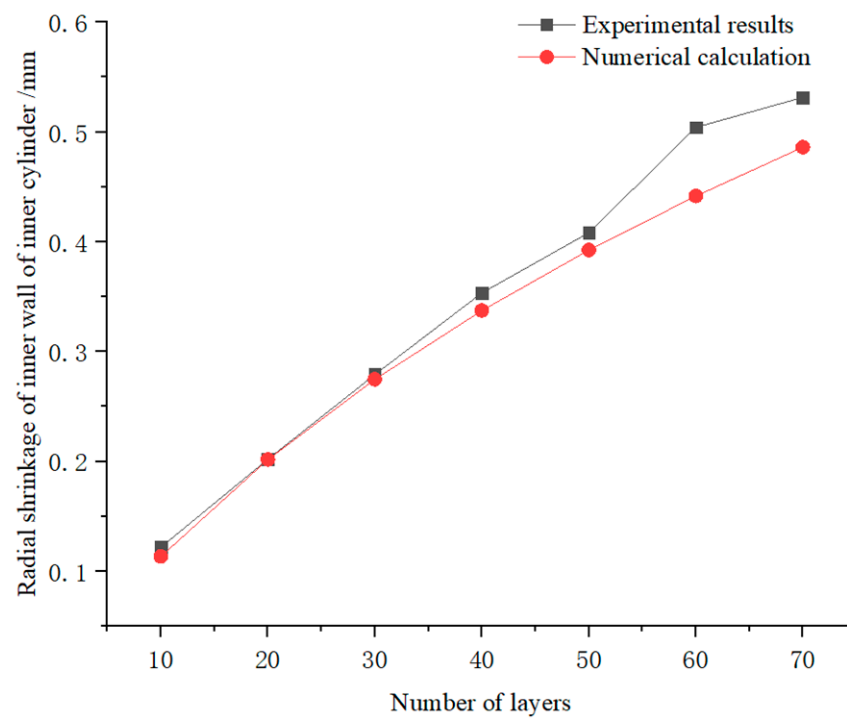
The previous two sets of model parameters can be substituted into the mathematical model described in Section 2.2 to calculate the corresponding radial shrinkage and compare it with the experimental results in the literature. The relevant data are shown in Tables 3 and 4, and are plotted in Figures 5 and 6. Through comparison and calculation, the maximum error of the two groups of data is 4.08%, which indicates that the mathematical model has high accuracy.

**Table 3.** Comparison of the radial shrinkage results of the first group of models.

Number of Layers	Radial Shrinkage of Inner Wall of Inner Cylinder/mm	
	The Experimental Data from the Xi'an Heavy Machinery Research Institute	Numerical Model in This Study
10	0.121800	0.1133
20	0.201975	0.2017
30	0.279150	0.2748
40	0.353475	0.3374
50	0.408375	0.3925
60	0.504300	0.4417
70	0.531750	0.4863

**Table 4.** Comparison of the radial shrinkage results of the second group of models.

Number of Layers	Radial Shrinkage of Inner Wall of Inner Cylinder/mm	
	The Experimental Data from the Xi'an Heavy Machinery Research Institute	Numerical Model in This Study
10	0.121800	0.1112
20	0.213900	0.1961
30	0.288000	0.2655
44	0.373920	0.3459
54	0.425880	0.3950
64	0.473040	0.4389
74	0.513840	0.4787
84	0.552000	0.5151
92	0.581880	0.5421
96	0.595320	0.5550

**Figure 5.** Shrinkage curves of the first group of models.

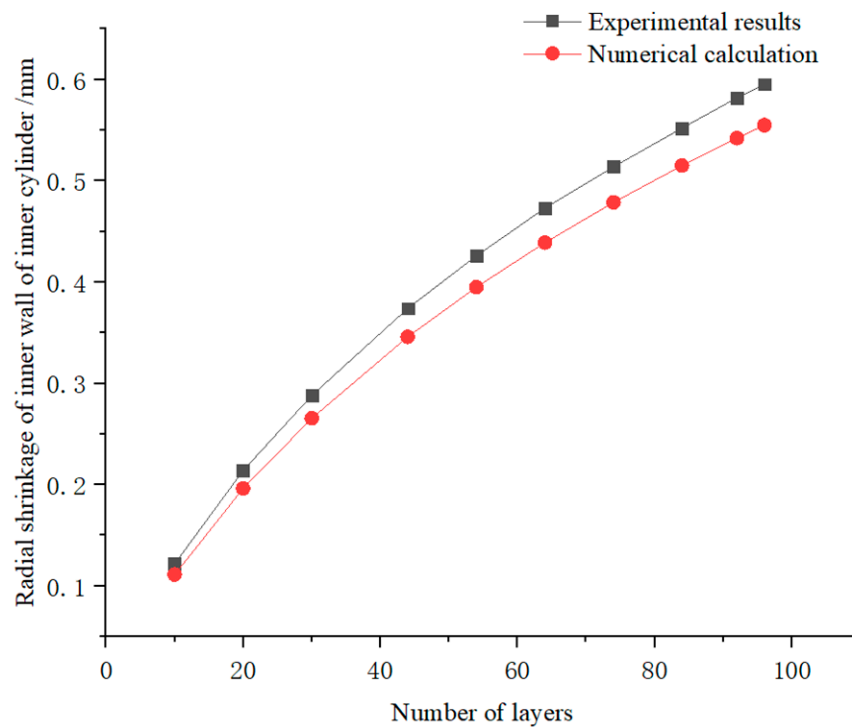


Figure 6. Shrinkage curves of the second group of models.

#### 4. The Selection of the Design Scheme of the Ultrahigh-Pressure Hydrostatic Extrusion Cylinder

In this section, mathematical optimization models for the three-layer combined extrusion cylinder and the single-layer core steel-wire-winding extrusion cylinder are established based on the mechanical model mentioned earlier. Additionally, the bearing capacities are compared, which will serve as the basis for the selection of the ultrahigh-pressure extrusion cylinder. Other elements, such as the wire-winding mode and the number of core layers of the wire-winding-type ultrahigh-pressure extrusion cylinder, are discussed further.

##### 4.1. Comparative Study of the Design of the Ultrahigh-Pressure Extrusion Cylinder

Because the cost of the extrusion cylinder is extremely expensive, it is very important to choose the most suitable structure for the ultrahigh-pressure extrusion cylinder while considering its processing and manufacturing difficulties. In this study, the optimal scheme is determined by comparing the minimum outer diameter required by the widely used three-layer prestressed composite extrusion cylinder and the single-layer cored steel-wire-winding extrusion cylinder for the same internal pressure. Figure 7 shows the schematic diagram of the two types of extrusion cylinders.

The internal pressure is 1500 MPa and the inner diameter radius is 110 mm. The elastic modulus  $E$  is 210 GPa and Poisson's ratio  $\mu$  is 0.3. The safety factor of the design of the extrusion cylinder is 1.3, the allowable stresses of the core cylinder and the steel wire are 1334 MPa and 1050 MPa, respectively, and the third strength theory is used for the strength calibration [23]. To compare the ultimate bearing capacity of the composite cylinder and the steel-wire-winding extrusion cylinder, the optimal design scheme of the ultrahigh-pressure extrusion cylinder is selected. Based on the principle of equal-strength design, a mathematical optimization model is proposed for comparative analysis.

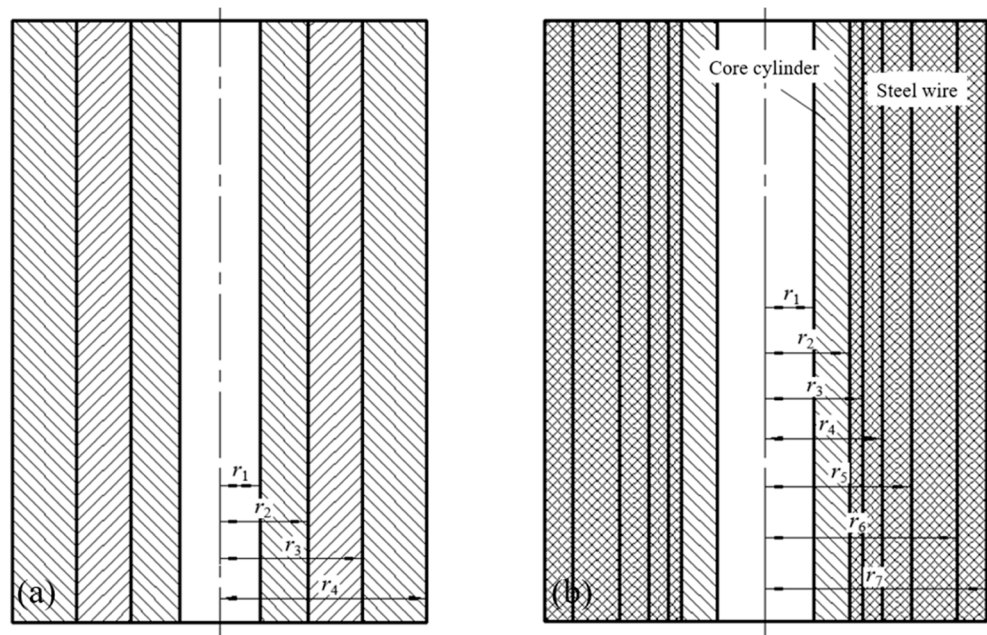


**Figure 7.** Schematic diagram of cylinders: (a) three-layer combined cylinder; (b) steel-wire-winding cylinder.

4.1.1. Mathematical Optimization Model

For the specific internal pressure and inner diameter conditions, the minimum outer diameter for which the extrusion cylinder can bear the corresponding load satisfies the design principle of equal strength and the constraint conditions. For this nonlinear multi-objective optimization problem, the *fmincon* function in the MATLAB optimization toolbox is adopted, and the calling format is

$$[x, fval, exitflag] = fmincon(fun, x0, A, Aeq, beq, ib, ub, nonlcon, options). \quad (6)$$

For the extrusion cylinder after assembly, the inner diameter of the *i*-layer cylinder is  $R_{i, in}$  and the outer diameter is  $R_{i, out}$ . The inner and outer wall pressures subjected to this are  $P_{i-1, i}$  and  $P_{i, i+1}$ , respectively. The strength of the extrusion cylinder calculated with the Tresca criterion is  $\sigma_i$ .

The constraint conditions are as follows:

1. Intensity check. Both the core cylinder layer and the steel wire layer should meet the strength condition—that is, the stress intensity value calculated with the Tresca criterion should not exceed the allowable stress.
2. Instability check. The conditions under which the cylinder does not destabilize under external pressure. In other words, the external pressure of each layer should not exceed the ultimate external pressure of the layer, and the safety factor is set to 2.

The mathematical optimization models of the three-layer combined extrusion cylinder and the single-layer core steel-wire-winding extrusion cylinder are shown in Tables 5 and 6.

**Table 5.** Optimization model of three-layer combined extrusion cylinder.

Three-Layer Combined Extrusion Cylinder	Mathematical Expression
Object function	$\min f(\max[\sigma_1, \sigma_2, \sigma_3]), \min(r_o)$
Variables	$r_{1,in} \ r_{1,out} \ r_{2,in} \ r_{2,out} \ r_{3,in} \ r_{3,out} \ P_{12} \ P_{23}$
Strength check	$\sigma_1 < [\sigma_1], \sigma_2 < [\sigma_2], \sigma_3 < [\sigma_3]$
Instability of checking	$P_{12} \leq \frac{E}{1-\mu^2} \left( \frac{r_{2,out}^2 - r_{1,in}^2}{r_{1,out}^2 + r_{1,in}^2} \right)^3, P_{23} \leq \frac{E}{1-\mu^2} \left( \frac{r_{2,out}^2 - r_{2,in}^2}{r_{2,out}^2 + r_{2,in}^2} \right)^3$

**Table 6.** Optimization model of single-layer steel-wire-winding extrusion cylinder.

Three-Layer Combined Extrusion Cylinder	Mathematical Expression
Object function	$\min f(\max[\sigma_1, \sigma_{s1}, \sigma_{s2}, \sigma_{s3}, \sigma_{s4}, \sigma_{s5}], \min(r_o))$
Variables	$r_{1,in} \ r_{1,out} \ P_{i-1,1} \ P_{i,j+1} \ (i = 1, 2, 3, 4, 5, 6)$
Strength check	$\sigma_1 < [\sigma], \sigma_{si} < [\sigma_s] \ (i = 1, 2, 3, 4, 5)$
Instability of checking	$P_{i,j+1} \leq \frac{E}{1-\mu^2} \left( \frac{r_{i+1}^2 - r_i^2}{r_{i+1}^2 + r_i^2} \right)^3 \ (i = 1, 2, 3, 4, 5)$

4.1.2. Comparison and Analysis of Design Schemes

With the optimization model established earlier, the optimization calculation for the three-layer combined extrusion cylinder and the single-core steel-wire-winding extrusion cylinder is carried out. As discussed, the inner wall radius is set to 110 mm, and the minimum outer diameters of the two extrusion cartridges for the same determined internal pressure are calculated. The internal pressure  $P$  is the abscissa and the outer diameter  $R$  is the ordinate, as shown in Figure 8.

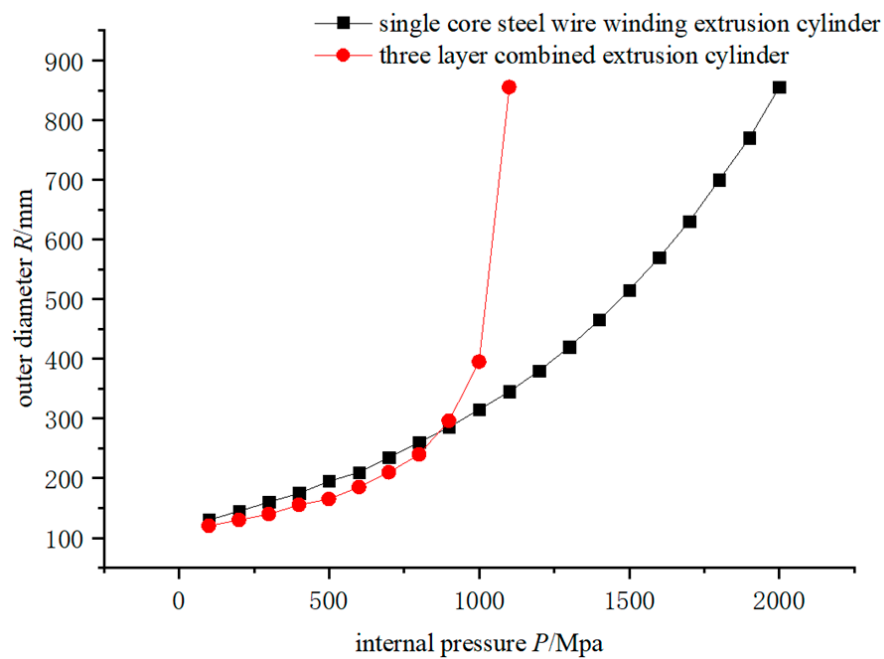


**Figure 8.** Comparison of structure scheme of three-layer combined cylinder and single-layer steel-wire-winding cylinder.

As shown in the figure, when the inner diameter is 110 mm, the intersection point of the three-layer combined extrusion cylinder and the single-layer core steel-wire-winding extrusion cylinder is about 850 MPa. That is, when the internal pressure is low, the three-layer combined extrusion cylinder has a better bearing capacity. In addition, Yan and Yu [23] mentioned that when the ratio of the outer diameter to the inner diameter of a multilayer combined extrusion cylinder is greater than 4, the pre-tightening force is limited in its ability to improve the bearing capacity of the extrusion cylinder. As shown in Table 7, the results of this study are consistent with this concept. For an ultrahigh-pressure interval greater than the critical internal pressure value, it is obvious that the steel-wire-winding extrusion cylinder is more suitable for use in the structural design scheme of the ultrahigh-pressure extrusion cylinder.

**Table 7.** Ratio of the outer diameter to the inner diameter of the three-layer combined cylinder and the single-layer steel-wire-winding cylinder.

Internal Pressure/MPa	Ratio of Outside Diameter to Inside Diameter ( $r_o/r_i$ )	
	Three-Layer Combined Extrusion Cylinder	Single-Core Steel-Wire-Winding Extrusion Cylinder
100	1.09	1.18
200	1.18	1.32
300	1.27	1.45
400	1.41	1.59
500	1.50	1.77
600	1.68	1.91
700	1.91	2.14
800	2.18	2.36
900	2.69	2.59
1000	3.59	2.86
1100	7.77	3.14

#### 4.2. Structural Analysis of a Steel-Wire-Winding Type of Ultrahigh-Pressure Extrusion Cylinder

##### 4.2.1. Analysis of Winding Mode

According to the different requirements and working conditions, the wire-winding methods of a wire-winding type of extrusion cylinder can be divided into equal-shear-stress winding and equal-tension winding.

A large number of studies and facts have shown that the failure of steel wire is mainly caused by shear failure, not by excessive normal stress. Therefore, using the equal-shear-stress winding method based on the first strength theory is not suitable. In addition, equal-shear-stress winding is a relatively ideal winding mode that requires the tension of each layer of steel wire to be in a continuous state, and the construction is difficult. In fact, the equal-shear-stress winding construction adopts the hierarchical form of equal tension in which the whole steel wire layer is divided into several “stages” of equal-tension winding [23]. In this chapter, an analysis is carried out and a comparison is made between the completely equal-tension winding method, that is, the equal-tension winding method mentioned earlier, and the hierarchical equal-tension winding method. Then, the most appropriate winding method is selected to carry out stress analysis and parameter optimization for the extrusion cylinder.

For constant-tension winding, this is a scheme of wrapping the outer shell of a core with constant initial stress. The process is relatively simple and widely used. The initial stresses of all steel wire layers with completely equal tension are the same, and this method is suitable for a situation with low internal pressure and fewer steel wire layers. However, the graded iso-tension has better adaptability and can withstand a higher internal pressure. The tension of the winding wire layer stress is shown in Figure 9. An arbitrary radius of the layer of steel wire  $r$  is set. The layer of steel wire uses the initial stress of  $\sigma_0$ . When the steel wire runs from  $r$  to  $r_o$ , there is a layer of steel wire under the outer tangential compressive stress of the steel wire  $\sigma'_{gt}$ , the radial compressive stress  $\sigma_{gr}$ , the winding layer after the completion of the steel wire radial compressive stress  $\sigma_{gr}$ , and tangential tensile stress  $\sigma_{gt}$ .

By definition,

$$\sigma_{gt} = \sigma_0 - \sigma'_{gt}. \quad (7)$$

As shown in Figure 9, a micro-element with the angle  $d\theta$  and the internal and external radius  $r$  and  $r + dr$  is constructed inside the steel wire layer. According to the balance of the micro-element, the following expression is obtained:

$$(\sigma_{gr} + d\sigma_{gr})(r + dr)d\theta - \sigma_{gr}rd\theta + 2 \cdot \sigma_{gt}dr \sin \frac{d\theta}{2} = 0. \quad (8)$$

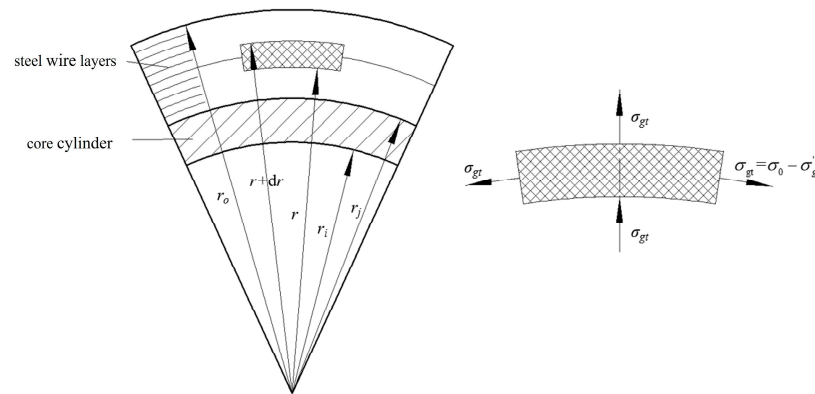


**Figure 9.** Stress analysis of micro-element of steel wire layer.

When  $\theta \rightarrow 0$ ,  $\sin \frac{d\theta}{2} \approx \frac{d\theta}{2}$ . Then, the higher-order term is omitted, and

$$\sigma_{gr} + \sigma_{gt} + r \frac{d\sigma_{gr}}{dr} = 0. \quad (9)$$

In addition, according to the Lamé formula for external pressure alone,

$$\sigma'_{gt} = \sigma_{gr} \frac{r^2 + r_i^2}{r^2 - r_i^2}. \quad (10)$$

By substituting Equations (7) and (10) into Equation (9), the general solution formula for a radial force on the radius in a pre-tightening state can be obtained as follows:

$$\sigma_{gr} = \frac{r^2 - r_i^2}{r^2} \left[ C - \frac{\sigma_0}{2} \ln(r^2 - r_i^2) \right]. \quad (11)$$

Figure 10 shows the comparison results for the bearing capacities of the single-layer cylinder complete constant-tension winding model and the single-layer cylinder graded constant-tension winding model when the inner diameters are both 110 mm. In the low-pressure range, the complete constant-tension winding method is slightly better than the graded constant-tension winding method. However, as the pressure increases, its bearing capacity is not as good as that of the hierarchical equal-tension winding method. Because the initial stresses in the equal-tension winding mode are all the same, as the thickness of the steel wire layer increases, the steel wire on the outside cannot play a pre-tightening role; that is, the pre-tightening role of the steel wire layer cannot be fully enacted. This problem can be solved by adjusting the initial stress of each “stage” of the steel wire layer. Therefore, for the selection of the winding mode of the wire-winding-type ultrahigh-pressure extrusion cylinder, the graded constant-tension winding method is adopted in this study.

#### 4.2.2. Core–Shell Layer Analysis

In recent years, because of the urgent development of ultrahigh-pressure hydrostatic extrusion technology, it has been necessary to improve its carrying capacity and ensure it has a long service life. Compared with a single-layer core-cylinder wire-winding extrusion cylinder, the inner core cylinder of a multilayer core-cylinder wire-winding extrusion cylinder is replaceable; so, the technology got multilayer core-cylinder wire winding can be developed. To quantitatively analyze the influence of the number of cores on the bearing capacity of a wire-winding extruded cylinder, the ultimate bearing capacities of a single-core cylinder, a double-core cylinder, and a three-core cylinder are analyzed and compared. The analysis and comparison are used as the theoretical basis for selecting the appropriate number of cores for a wire-winding ultrahigh-pressure extruded cylinder. The inner diameter of the extrusion cylinder is limited to 110 mm, and the outer diameter of each type of extrusion cylinder for the same internal pressure is calculated. The results are shown in Figure 11.

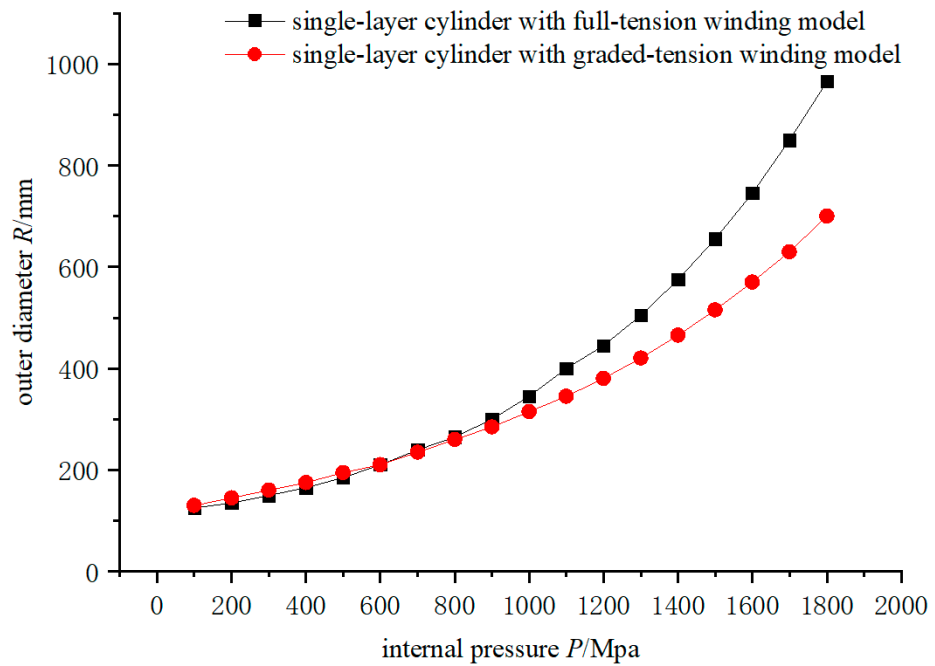


**Figure 10.** Comparison of single-layer cylinder with full-tension winding model and single-layer cylinder with graded-tension winding model.

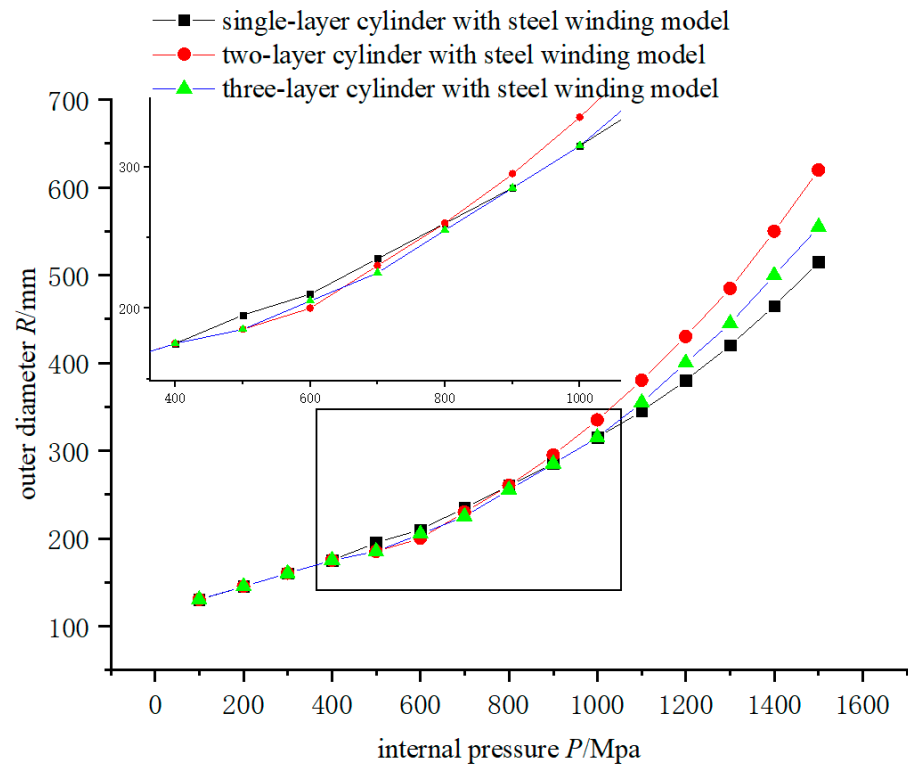


**Figure 11.** Comparisons of the single-layer cylinder with the steel-wire-winding model, the two-layer cylinder with the steel-wire-winding model, and the three-layer cylinder with the steel-wire-winding model.

When the internal pressure is less than 400 MPa, the bearing capacities of the three types of wire-winding extrusion cylinders are similar. However, when the internal pressure is within the range of 400 MPa to 1000 MPa, the three-layer wire-winding-type cylinder has a better effect. When the internal pressure exceeds 1000 MPa, the advantages of the

single-layer wire-winding-type cylinder are reflected. Although the allowable strength of the thick-walled cylinder is higher than that of the steel wire layer—that is, although the thick-walled cylinder can bear a higher pressure under the condition of the same wall thickness—the problem of instability occurs when the external force is too large. However, when the internal pressure is large, the preloading force on the outer layer of the core cylinder is also increased, and an inner lining with a larger wall thickness is needed for the multilayer winding model. With an increase in the wall thickness of the middle lining, its pre-tightening effect on the inner cylinder is reduced. Therefore, when the internal pressure is large, the single-layer cylinder winding model with the same internal pressure is superior to the multilayer cylinder winding model.

## 5. Discussion

In this study, we established the mechanics model of a multilayer combined extrusion cylinder based on the interfacial force calculated by Song [8]. In addition, we derived the mechanics model of a steel-wire-winding extrusion cylinder according to a previous elastic–plastic theory [1]. Compared with earlier steel-wire-winding calculation methods [14,23], the method described in this paper is more concise. The finite element method and the experimental data were used to verify the theoretical calculation results. According to these results, a mathematical optimization model was built for the exploration of the ultimate bearing capacity and its influential factors, such as the winding mode and the number of core layers, which was similar to the work of Chi and Cao [13]. Currently, the production and application of ultrahigh-pressure hydrostatic extrusion technology are limited, being restricted primarily by the design and manufacture of ultrahigh-pressure extrusion cylinders. This research on the basic design theory and selection criterion for ultrahigh-pressure cylinders is important for the popularization and application of ultrahigh-pressure hydrostatic extrusion technology. Therefore, the related work in this study has important theoretical guiding significance and practical value to supplement the limited research available on the design mechanism and selection of ultrahigh-pressure extrusion cylinders.

## 6. Conclusions

In this paper, we propose a feasible selection method for an ultrahigh-pressure extrusion cylinder. By calculating the ultimate bearing capacity of the extrusion cylinder for a specific outer diameter, two main design schemes and different structure forms are compared. For an ultrahigh-pressure hydrostatic extrusion cylinder in which the internal pressure is greater than 1000 MPa, a single-layer cylinder with graded-tension wire winding is determined to be the better choice. Notably, the proposed method and mentality take advantage of the selection of an ultrahigh-pressure extrusion cylinder before the design process, which can save large amounts of time and economic costs. We evaluated our theoretical models using an extensive finite element analysis and experiments. The results show that the deviation of our theoretical models is within the acceptable limits.

This study, however, also has some limitations. Some deviations between the theoretical model and the actual working conditions exist, and the optimal design model of the extrusion cylinder needs to be improved for greater accuracy and ease of use.

Therefore, this work has several interesting research directions. First, the calculation models presented in this paper have room for further refinement because of the ideal hypotheses. Second, in addition to the comparison of the ultimate bearing capacities of the main design schemes of extrusion, we would like to develop a wide-ranging diagram for selection that includes many kinds of extrusion cylinders and their different structure forms.

**Author Contributions:** Conceptualization, J.Y. and L.Z.; writing—original draft preparation, J.Y.; writing—review and editing, L.Z.; methodology, J.Z.; validation, H.W. and D.Z.; supervision, Y.L.; funding acquisition, Y.W. All authors have read and agreed to the published version of the manuscript.

**Funding:** This study was funded by Shanxi Provincial Key Research and Development Project (2018GY-194) and open topic of the State Key Laboratory of Metal Extrusion and Forge Equipment Technology(1042012920180092).

**Data Availability Statement:** Data will be made available on request.

**Conflicts of Interest:** The authors declare no conflict of interest.

## References

1. Horne, R.M. The Elastic-Plastic Theory of Containers and Liners for Extrusion Presses. *Proc. Inst. Mech. Eng.* **1955**, *169*, 107–122. [[CrossRef](#)]
2. Zhao, Y.L.; Liu, J.A. The optimal design of extrusion cylinder (1). *Light Alloy Fabr. Technol.* **1996**, *6*, 34–41.
3. Ao, W.G.; Wang, X. The radius and interference of prestressed composite cylinders are analyzed by unified strength theory. *J. Chongqing Technol. Bus Univ. Sci. Technol.* **2011**, *28*, 284–288.
4. Wang, Y.; Liu, Q.K.; Wang, L.G. Numerical Simulation and Theoretical Verification of Multi-layer Prestressed Cylinder. *Mech. Eng.* **2002**, *12*, 9–12.
5. Li, Y.; Liu, Q.K.; Wang, L.G.; Wang, Y. Analysis of the regularity of deformation and stress distribution of multi-layer circular extrusion container. *J. Hefei Univ. Technol. Sci. Technol.* **2002**, *6*, 1154–1158.
6. Tang, B.N.; Guo, C.H.; Bao, D.N.; Li, J.L. Simplified Design of Extrusion Press Container. *Nonferrous Met. Eng. Res.* **2011**, *32*, 13–15.
7. Xiong, Y.K. The Effect on Usage of Multi-Layers Container with Autofrettage Technology. Master's Thesis, Chongqing University, Chongqing, China, 2013.
8. Song, Z.T. Mechanism and Life Prediction of Creep Fatigue Damage under the Complex Service Condition of the Large Extrusion Cylinder. Master's Thesis, Chongqing University, Chongqing, China, 2015.
9. Li, Y.H. Study on the Influence of Material Creep on the Excess Surplus of the Extrusion Tube in the Service Environment. Master's Thesis, Chongqing University, Chongqing, China, 2017.
10. Ma, L.; Luo, Y.X.; Song, Z.X.; Wang, Y.Q. Design Theory and Lifetime Prediction of Extrusion Container Subjected to Creep-fatigue Interaction. *J. Mech. Eng.* **2017**, *53*, 163–172. [[CrossRef](#)]
11. Wu, R.D.; Wang, X.F.; Zhang, L. Prestressed steel wire winding splitt-assembled extrusion cylinder. *J. Tsinghua Univ. Sci. Technol.* **2010**, *50*, 974–979.
12. Yang, Y.F.; Li, M.Z.; Liu, Z.W.; Wang, B.L. Structure of Wire Winded Extrusion Container and the Analysis of the Pre-stressed Winding Layer. *J. Mech. Eng.* **2015**, *51*, 89–94. [[CrossRef](#)]
13. Chi, Y.C.; Cao, J.G. Investigation on the prestress of the external steel-wire winding on the split-assembled extrusion cylinder. *J. Inn. Mong. Univ. Sci. Technol.* **2013**, *32*, 137–139.
14. Liu, C.Y.; Zhang, L.; Lin, F.; Zhang, R.J.; Yan, Y.N.; Kang, F.Y. Design of Steel Wire Wound Extrusion Containers for Steel Hot Extrusion Process. *J. Mech. Eng.* **2013**, *49*, 78–83. [[CrossRef](#)]
15. Vedeld, K.; Sollund, H.A. Stresses in heated pressurized multi-layer cylinders in generalized plane strain conditions. *Int. J. Press. Vessel. Pip.* **2014**, *120*, 27–35. [[CrossRef](#)]
16. Sollund, H.A.; Vedeld, K.; Helleland, J. Efficient analytical solutions for heated and pressurized multi-layer cylinders. *Ocean. Eng.* **2014**, *92*, 285–295. [[CrossRef](#)]
17. Zhang, Z.; Zhou, W.; Shi, Z.; Lin, J. Investigation of die designs on welding quality and billet material utilisation for multi-container extrusion of wide stiffened aluminium panels. *Int. J. Adv. Manuf. Technol.* **2023**, *127*, 4149–4162. [[CrossRef](#)]
18. Zhang, Z.; Zhou, W.; Shi, Z.; Lin, J. Advances on manufacture methods for wide lightweight aluminium stiffened panels. In *IOP Conference Series: Materials Science and Engineering*; IOP Publishing: Bristol, UK, 2022; Volume 1270, p. 012122.
19. Ma, M. Cumulative damage in fatigue. *J. Appl. Mech.* **1945**, *67*, A159–A164.
20. Luo, Y.; Xiong, Y.; Wang, Y.; Ma, L. A new model for predicting of stresses on the compound extrusion container. *WSEAS Trans. Appl. Theor. Mech.* **2014**, *9*, 229–237.
21. Duan, L.H. Research on Deformation Analysis and Structure Optimization of Inner Hole of Extrusion Cylinder. Master's Thesis, Chongqing University, Chongqing, China, 2012.
22. Wang, Y.Q.; Li, L.; Yan, X.C.; Luo, Y.X.; Wu, L. Modeling of Stress Distribution During Strip Coiling Process. *J. Iron Steel Res. Int.* **2012**, *19*, 6–11. [[CrossRef](#)]
23. Yan, Y.N.; Yu, X.L. *Prestressed Structures in Mechanical Design*; China Machine Press: Beijing, China, 1989.

**Disclaimer/Publisher's Note:** The statements, opinions and data contained in all publications are solely those of the individual author(s) and contributor(s) and not of MDPI and/or the editor(s). MDPI and/or the editor(s) disclaim responsibility for any injury to people or property resulting from any ideas, methods, instructions or products referred to in the content.